

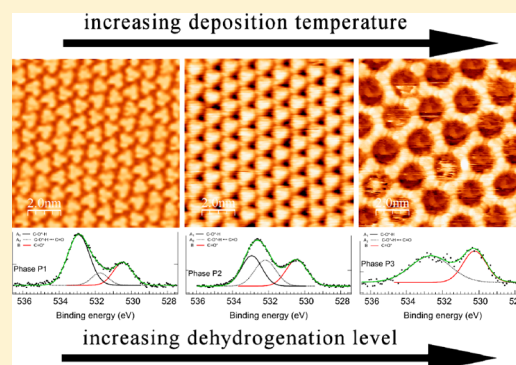
Combined Photoemission Spectroscopy and Scanning Tunneling Microscopy Study of the Sequential Dehydrogenation of Hexahydroxytriphenylene on Ag(111)

Luca Giovannelli,^{*,†} Oualid Ourdjini,[†] Mathieu Abel,[†] Rémy Pawlak,^{†,§} Jun Fujii,[‡] Louis Porte,[†] Jean-Marc Themlin,[†] and Sylvain Clair^{*,†}

[†]Aix Marseille Université, CNRS, Université de Toulon, IM2NP UMR 7334, 13397 Marseille, France

[‡]INFN, CNR, TASC Lab, I-34012 Trieste, Italy

ABSTRACT: The structural evolution of 2,3,6,7,10,11-hexahydroxytriphenylene (HHTP) single-layer networks on Ag(111) was investigated by scanning tunneling microscopy and core-level photoemission. The molecules adsorbed in flat-lying conformation and formed well-ordered supramolecular domains. Three different phases were observed depending on the substrate temperature during deposition. Core-level photoemission showed that the radical changes in the supramolecular networks corresponded to different degrees of dehydrogenation of the six-fold hydroxyl functional groups borne by the molecule. Remarkably, hydroxyl groups involved in strong H bonding with carbonyl oxygens appeared as distinct components in the O 1s spectra.



INTRODUCTION

Supramolecular self-assembly of organic molecular layers has focused an impressive scientific effort in recent years^{1,2} that stems from the variety and versatility of noncovalent interactions (van der Waals, H-bond, metal–ligand), sustaining the formation of extended well-defined nanostructures. The a priori design of the precursor molecules seen as “building block” and the anchoring of functional groups are of prime importance to create the final superstructure and the desired properties. However, in some cases, the molecules undergo chemical modifications after deposition on a reactive substrate. In particular, deprotonation or dehydrogenation reactions can occur readily on metal surfaces, as it was shown, for example, for carboxylic acids,^{3–7} amines^{8,9} or alcohols.^{10–14} In most cases, the chemical transformation induces strong modifications in the self-assembly processes and the resulting superstructure by allowing new bonding configurations, both between molecules (new hydrogen bonds) as well as with the underlying substrate or with adatoms.

A thorough comprehension of the mechanisms governing molecular self-assembly can hardly be achieved without employing complementary experimental techniques. In this perspective, combining atomic scale scanning tunneling microscopy (STM) observations and photoemission spectroscopy is demonstrated to be a valid approach.¹⁵ Thanks to its high sensitivity to subtle changes of the charge distribution around a given atomic species, photoemission spectroscopy has been successfully used to study noncovalent intermolecular interactions including their impact on the evolution of the self-assembly properties. The H-bonding picture could be

established by determining the chemical state of the periphery groups (e.g., deprotonation of carboxylic acids transforming to carboxylate^{3–7}) or directly by addressing the more elusive, chemically shifted donor and acceptor components. The latter have been singled out for instance in the case of isonicotinic acid¹⁶ on Ag(111) or benzoic acid on Au(111).¹⁷

The present work combines STM and X-ray photoelectron spectroscopy (XPS) to study the various self-assembled networks formed by the molecule 2,3,6,7,10,11-hexahydroxytriphenylene (HHTP)^{18,19} on the well-defined Ag(111) surface. HHTP is composed of a triphenylene core functionalized by six peripheral hydroxyl groups (Figure 1a) that govern the intermolecular interactions through the formation of hydrogen

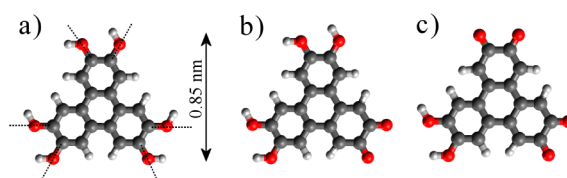


Figure 1. (a) Schematic drawing of 2,3,6,7,10,11-hexahydroxytriphenylene (HHTP). The dotted lines indicate rotational degrees of freedom for hydroxyl H atoms. As a result, a large number of conformations are allowed for this molecule. (b) Proposed conformation for the diketone derivative formed after dehydrogenation of HHTP. (c) Tetra-ketone derivative.

Received: February 21, 2014

Revised: June 17, 2014

Published: June 17, 2014

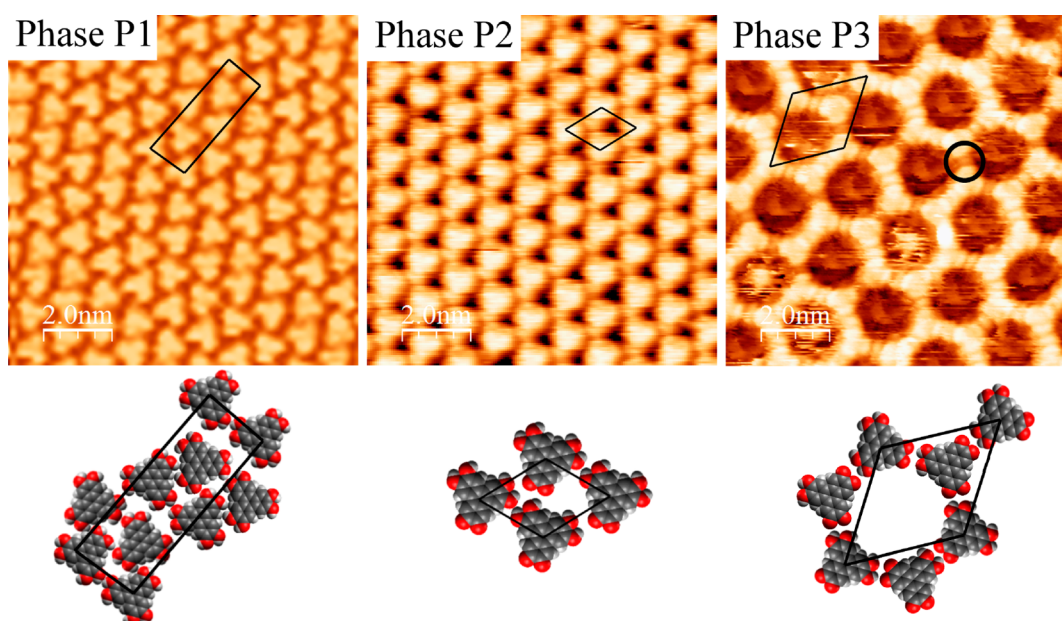


Figure 2. STM images and corresponding tentative models (bottom) of the three phases found for the system HHTP/Ag(111). (See the text for details.) For phase P3, the circle shows an intermolecular bonding with low electron density corresponding to bonding between two dihydroxyl groups.

bonds.^{11,20–23} When deposited on a hot surface, the hydroxyl moieties undergo partial dehydrogenation due to the catalytic activity of the metal substrate and transform into ketone groups; the higher the deposition temperature, the more advanced the dehydrogenation reaction. This chemical transformation implies important modifications of the intermolecular interactions (and thus the formation of different supramolecular phases).

EXPERIMENTS

The experiments were performed at room temperature in two separate UHV systems. The first comprises a preparation chamber and a multitechnique analysis chamber for STM and photoemission. The second is the APE experiment²⁴ at Elettra synchrotron light source (Trieste). The Ag(111) surface was prepared by repeated cycles of Ar⁺ sputtering and annealing. HHTP molecules (TCI Europe) were evaporated from a molybdenum crucible heated to a temperature of 500 K. The substrate temperature during deposition was kept constant, and the samples were cooled back to room temperature in ~30 min after deposition. STM experiments were recorded in the constant current mode with typical parameters $I_t = 0.2$ to 0.8 nA and $V_t = 0.8$ to 1.6 V. Images were partially treated with the free software WSXM.²⁵ XPS spectra were recorded by an EA125 Omicron electron energy analyzer in angular integrated mode (acceptance angle of 16°) using synchrotron X-rays of 700 eV and by standard Mg K- α source (photon energy of 1253.6 eV), resulting in an overall energy resolution of 0.3 and 1.1 eV, respectively. Sample degradation was avoided by reducing the exposure and measuring in different regions on the sample surface. All spectra were taken at room temperature in normal emission and are referenced in energy to the substrate Fermi level. Background-subtracted core-level spectra were fitted by a least-squares procedure using purely Gaussian peaks. Adding a Lorentzian convolution did not improve or alter the results of the fits.

RESULTS

STM Structural Characterization. HHTP forms extended supramolecular domains on the Ag(111) surface, as observed by STM at room temperature. All phases have been previously described,^{11,20,21} and their main characteristics are summarized here. The molecules appear as triangles, the size of which corresponds to individual molecules in a flat-lying configuration (~ 1 nm wide; see Figure 1). Depending on the substrate temperature during deposition (room temperature, 450 or 500 K), three distinct phases formed. (See Figure 2)

In the phase formed after room temperature deposition (P1), the molecules face each other, forming rows of dimers aligned with the substrate [110] high symmetry direction. The baseline of each triangle representing a single molecule is not perfectly aligned with the row direction but is rather slightly rotated by an angle of $\sim 10^\circ$. The direction of this misalignment is preserved along each dimer row but is opposite for adjacent rows. The periodic unit cell therefore comprises four molecules and corresponds to a $(4 \ 0 \ 1 \ 14)$ superstructure. This phase has a density of 0.99 molecules·nm⁻² and represents the densest network. The anisotropy of the phase is reproduced in the elongated shape of the molecular domains. Three equivalent orientational domains are found on the surface.

For a deposition on a substrate held at 450 K (phase P2), the molecules self-assemble in exact hexagonal domains with a mesh parameter of (1.1 ± 0.1) nm aligned with the [110] high-symmetry direction of the Ag substrate. The superstructure corresponds to a $p(4 \times 4)$ phase providing a density of 0.86 molecules·nm⁻², slightly lower than phase P1. Additionally, domain boundaries are formed regularly with a 22 nm period, thus forming a well-organized hexagonal supernet, as detailed in ref 20. In adjacent domains, the molecule orientation is rotated by 180° , and the structure of the domain boundaries is identical to the dimer row structure of phase P1. Again, the baseline of each triangle representing a single molecule is rotated by a small angle of $\sim 10^\circ$ with respect to the network direction. Because this off-axis angle is preserved in

adjacent domains (as is the case inside the dimer rows of phase P1), the chiral asymmetry is uniquely defined in a single superdomain. Superdomains with opposite chirality are equally found on the surface.

For a deposition on a substrate held at 500 K (phase P3), HHTP molecules form an open network with honeycomb structure.¹¹ The network has a periodicity of (2.2 ± 0.1) nm and forms an angle of $\sim 6^\circ$ with the [110] direction of the Ag(111) surface. Two distinct rotational domains are observed (corresponding to angles of $+6^\circ$ and -6°). The unit cell contains two molecules and forms a $(7\ 1, -1\ 8)$ superstructure. The density of this phase amounts to $0.48\text{ molecules}\cdot\text{nm}^{-2}$, which corresponds to the lowest density of the three phases. As previously reported,¹¹ this phase can form only if part of the molecules are dehydrogenated, that is, if some of the dihydroxyl groups transformed into diketone. More precisely, a mixture of di- and tetraketone molecules is necessary to construct the honeycomb network, ideally in a 1:1 ratio. However, STM data reveal, in general, a higher ratio (or lack of tetraketones, or insufficient dehydrogenation) by the presence of low electron density regions at the junction between two adjacent molecules. (See the circle in Figure 2.) Note that, in opposite, in the case of a too large excess of tetraketones with respect to diketones, attractive intermolecular interaction would vanish and the network would not form.

Core Levels. The O 1s XPS spectra for the different phases P1, P2, and P3, together with the spectrum of a thick film of HHTP, are displayed in Figure 3. The thick film presents a single component²⁶ (binding energy (BE) of 532.8 eV) that includes contributions from hydroxyl groups with different local environments involving hydrogen bonds.²⁷ Some of these bonds are established internally between adjacent hydroxyls of a given molecule and some also externally between neighboring molecules.

When considering the O 1s spectra of single-layer molecules, two peaks denoted as A and B are present for all structural phases. This clearly indicates a chemical modification of part of the hydroxyl groups. The high BE peak A (~ 532.8 eV) is due to intact hydroxyl sites. The low BE peak B (~ 530.3 eV) can be assigned to a partial dehydrogenation of the HHTP molecules, promoting a fraction of carbonyl groups.¹² Increasing the deposition temperature resulted in a progressive growth of the carbonyl component. The fraction of hydroxyls to carbonyls A/B gives the extent of dehydrogenation and can be evaluated quantitatively by a least-squared fitting procedure, as displayed in Figure 3, and whose results are summarized in Table 1.²⁸

High-resolution spectra performed for P1 and P2 reveal that the hydroxyl peak cannot be accounted for by a single component, and a second component A_2 was added to fit the asymmetry. Given its lower binding energy, this component was assigned to hydroxyl groups involved in strong hydrogen bonds with carbonyl oxygens. The structural analysis of phase P3 reveals that nearly all hydroxyls are bonded to carbonyl oxygens,¹¹ and a single component A_2 was therefore assigned for this phase. Comparatively, the width of carbonyl peak increases only slightly through phase transformations, suggesting a minor effect of H-bond formation on the acceptor groups.

DISCUSSION

We propose that the hydroxyl groups of HHTP undergoes a thermally activated dehydrogenation, which is initiated by the catalytic activity of the surface, thereby transforming into carbonyl groups. The resulting hydrogen atoms are expected to

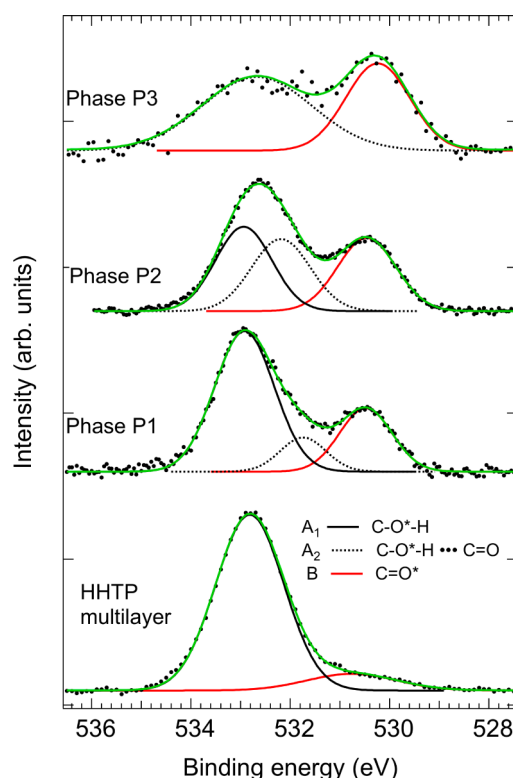


Figure 3. XPS core-level spectra of the O 1s region for the three different phases P1, P2, and P3 and the thick multilayer film of HHTP on Ag(111) showing the progressive dehydrogenation in the different phases (growth of carbonyl oxygen peak B at 530 eV, see Table 1). Two components at the hydroxyl peak A can be clearly distinguished for P1 and P2. The right component A_2 is assigned to hydroxyl groups involved in H bonding with carbonyl groups. The HHTP multilayer and phase P3 were measured with standard Mg K- α X-ray source.²⁸ The P1 and P2 spectra were measured with 700 eV synchrotron radiation. (See the text for details.)

recombine to form molecular hydrogen, which spontaneously desorbs from noble-metal substrates under the conditions employed.^{12,29,30} For stepwise removal of hydrogen atoms (sequential oxidation of hydroxyl groups), only an even number of dehydrogenation can deliver a stable derivative and thus respect all atoms valencies (formation of di- or tetra-ketones only, see Figure 1).¹¹ Carbonyl oxygen is measured in phase P1, meaning that the dehydrogenation reaction occurs already at room temperature. However, the large hydroxyl to carbonyl oxygen ratio found indicates that the reaction is inhomogeneous or incomplete. Indeed, the homogeneous formation of simply dehydrogenated HHTP (formation of diketone derivatives) would deliver a hydroxyl to carbonyl oxygen ratio of 2:1. The effective ratio of 3:1 measured for phase P1 thus corresponds roughly to a mixture of three diketone derivatives for one intact HHTP. The unit cell of this phase is composed of four distinct molecules. (See Figure 2) A composition of one HHTP and three diketone derivatives per unit cell gives a hydroxyl to carbonyl oxygen ratio of three, as found experimentally. For phase P2, the XPS spectrum can be simply interpreted as that of diketone molecules because the hydroxyl to carbonyl oxygen ratio is close to 2, although the presence of a stoichiometric mixture of intact HHTP and tetraketone molecules cannot be excluded. Finally, the component corresponding to carbonyl oxygens in the XPS spectrum increased considerably for phase P3, thus revealing a higher

Table 1. Results from the Deconvolution Analysis of the O 1s Peaks for the Three Different Phases and the Multilayer Thick Film^a

O 1s component	A ₁		A ₂		A ₂ /B	B		(A ₁ + A ₂)/B
O type	hydroxyl C–O–H		hydroxyl bonded to carbonyl C–O–H...			carbonyl C=O		hydroxyl/carbonyl ratio
	BE	fwhm	BE	fwhm		BE	fwhm	
P3	NA	NA	532.7	2.6		530.2	1.5	1.4
P2	532.9	1.3	532.2	1.4	1.0	530.5	1.4	2.1
P1	532.9	1.4	531.7	1.1	0.5	530.5	1.2	3.0
thick	532.8	1.6						

^aBinding energies (BE) and peak widths (fwhm) for the different oxygen types are reported. All values are in electronvolts. Component A₂ indicates chemically shifted hydroxyl donors bonded to carbonyl acceptors. The hydroxyl to carbonyl area ratios are also reported for the different phases.

degree of dehydrogenation. Indeed, the formation of a honeycomb network, as observed by STM, is only possible for a stoichiometric mixture of di- and tetraketones.¹¹ A close look into the STM images reveals that a “break” or a low-electron-density region (appearing as a dark region in the STM image) at the junction between two adjacent molecules can be occasionally observed (Figure 2), corresponding to particular bonding configurations between two dihydroxyl groups.¹¹ This observation reveals an excess of hydroxyl groups due to an excess of diketone derivatives as compared with tetraketone, in good agreement with the hydroxyl to carbonyl oxygen ratio of 1.4 measured by XPS (Table 1).

The substrate temperature during deposition thus controls the degree of oxidation of HHTP molecules and therefore the supramolecular structure. For intermediate temperatures below 500 K, mixtures of phases P1 and P2 can be observed and intermediate dehydrogenation levels are measured by XPS (data not shown). In the case of phase P3, the degree of oxidation of HHTP molecules is crucial, and a di- to tetraketone ratio very close to 1:1 is required. Higher dehydrogenation level prevents the formation of a supramolecular phase due to repulsion between ketone groups, and lower dehydrogenation induces molecular segregation and concomitant formation of phase P2. For these reasons, the deposition temperature range required to form phase P3 is rather narrow. Finally, the annealing time can also be a parameter accounting for the formation of the different phases, as the degree of advancement of the reaction is in part kinetically determined. In fact, postannealing was always much less efficient than controlling the deposition temperature to obtain pure phase monolayers.

As observed by the formation of three different phases, the degree of dehydrogenation of HHTP sensibly modifies the self-assembly properties in the monolayer regime and consequently also the intermolecular (H-bonding) configurations. The core-level chemical shift induced by H bonding in organic molecules has been studied both theoretically^{31–33} and experimentally^{16,17,34–36} on model systems. The creation of H bond induces withdrawing of charge from the donor and enrichment on the acceptor.³⁷ The combined effect of initial (electrostatic potential) and final (screening) state energies results in a stronger shift to lower BE for the donors as compared with the smaller shift to higher BE for the acceptors.^{31,33} As a result, the XPS BE difference between donor and acceptors groups reduces upon H-bond formation, with the reduction being more important for stronger H bonds.

The presence of H-bond donor and acceptor hydroxyl groups in the multilayer thick film^{18,19} produces a single component peak in O 1s spectrum. For single-layer phases the

formation of strong H bonds with carbonyl groups between partially dehydrogenated molecules is revealed by the presence of a second hydroxyl component A₂ at lower BE. The intensity of this component increases from phase P1 to P2, in parallel with the increased dehydrogenation and the creation of carbonyl oxygens. For P2, the BE of A₂ is slightly larger than for P1, which is indicative of a slightly weaker H bonding. This may result from larger H-bond lengths or a different interaction of the oxygens with the substrate.¹² The ratio between hydroxyls involved in H bonds with carbonyls versus carbonyls (A₂/B) is close to 1 for P2, whereas it is 0.5 for P1. In the latter phase, only a fraction of the carbonyls are thus involved in H bonds. For P3, most hydroxyls are engaged in H bonds with carbonyl groups, as expected from the structural model, and a single component was thus assigned for hydroxyl oxygens. The larger peak width measured reveals large heterogeneities in the bonding configurations of this phase. Moreover, the peak comprises additional contributions from the hydroxyl groups that are in excess with respect to carbonyl groups and that could not be explicitly determined. Additional broadening probably arises due to the two nonequivalent adsorption sites for the two molecules in the unit cell of this honeycomb network or also to a diffuse strain relaxation in the film.

The precise positions of the hydroxyl and carbonyl groups and the related configuration of intermolecular H bonds between the molecules could not be unequivocally established in structural models due to the large number of possibilities. (There are several dehydrogenated isomers and a rotational degree of freedom for each hydroxyl groups.) The high complexity of this system and the multiple H-bonding pattern possibilities probably contribute to the broadening of the XPS component A₂ in phases P2 and P3. Note that similar phases to P1 and P2 were found on a Au(111) surface,²² in which, however, no dehydrogenation was assumed.

CONCLUSIONS

We have studied the different phases formed by the molecule HHTP deposited on Ag(111) in submonolayer regime depending on the deposition temperature in the range 298 (RT) to 500 K. The structural properties were characterized by STM, while photoemission spectroscopy allowed characterization of the chemical states of the molecules. We found that partial dehydrogenation of the hydroxyl groups and formation of ketone derivatives already occurred at room temperature. Increasing deposition temperature resulted in an increase in the dehydrogenation rate, up to a di- to tetraketone molecule ratio close to 1 for deposition at 500 K. Remarkably, we observed a gradual decrease in the molecular density with increasing deposition temperature and increasing dehydrogenation. The

hydroxyl groups involved in strong H-bonding to carbonyl oxygens appeared as a distinct component in core-level photoemission O 1s region. Our combined STM and photoemission spectroscopy approach of this complex system thus appeared very efficient for extracting important parameters that govern the self-assembly processes of molecular systems on surfaces.

AUTHOR INFORMATION

Corresponding Authors

*L.G.: E-mail: luca.giovanelli@im2np.fr.

*S.C.: E-mail: sylvain.clair@im2np.fr.

Present Address

[§]R.P.: University of Basel, Department of Physics, Klingelbergstr. 82, CH-4056 Basel, Switzerland.

Notes

The authors declare no competing financial interest.

ACKNOWLEDGMENTS

This work has been carried out thanks to the support of the A*MIDEX project (no. ANR-11-IDEX-0001-02) funded by the Investissements d'Avenir French Government program, managed by the French National Research Agency (ANR).

REFERENCES

- (1) Barth, J. V. Molecular architectonic on metal surfaces. *Annu. Rev. Phys. Chem.* **2007**, *58*, 375–407.
- (2) Liang, H.; He, Y.; Ye, Y. C.; Xu, X. G.; Cheng, F.; Sun, W.; Shao, X.; Wang, Y. F.; Li, J. L.; Wu, K. Two-dimensional molecular porous networks constructed by surface assembling. *Coord. Chem. Rev.* **2009**, *253*, 2959–2979.
- (3) Stepanow, S.; Strunskus, T.; Lingenfelder, M.; Dmitriev, A.; Spillmann, H.; Lin, N.; Barth, J. V.; Woll, C.; Kern, K. Deprotonation-driven phase transformations in terephthalic acid self-assembly on Cu(100). *J. Phys. Chem. B* **2004**, *108*, 19392–19397.
- (4) Canas-Ventura, M. E.; Klappenberger, F.; Clair, S.; Pons, S.; Kern, K.; Brune, H.; Strunskus, T.; Woll, C.; Fasel, R.; Barth, J. V. Coexistence of one- and two-dimensional supramolecular assemblies of terephthalic acid on Pd(111) due to self-limiting deprotonation. *J. Chem. Phys.* **2006**, *125*, 184710.
- (5) Kanninen, L.; Jokinen, N.; Ali-Loytty, H.; Jussila, P.; Lahtonen, K.; Hirsimäki, M.; Valden, M.; Kuzmin, M.; Parna, R.; Nommiste, E. Adsorption structure and bonding of trimesic acid on Cu(100). *Surf. Sci.* **2011**, *605*, 1968–1978.
- (6) Faraggi, M. N.; Rogero, C.; Arnau, A.; Trelka, M.; Ecija, D.; Isvoranu, C.; Schnadt, J.; Marti-Gastaldo, C.; Coronado, E.; Gallego, J. M.; et al. Role of deprotonation and Cu adatom migration in determining the reaction pathways of oxalic acid adsorption on Cu(111). *J. Phys. Chem. C* **2011**, *115*, 21177–21182.
- (7) Erlep, T.; Shavorskiy, A.; Zheleva, Z. V.; Held, G.; Kalashnyk, N.; Ning, Y. X.; Linderöth, T. R. Global and local expression of chirality in serine on the Cu{110} surface. *Langmuir* **2010**, *26*, 18841–18851.
- (8) Lin, Y. P.; Ourdjini, O.; Giovanelli, L.; Clair, S.; Faury, T.; Ksari, Y.; Themlin, J. M.; Porte, L.; Abel, M. Self-assembled melamine monolayer on Cu(111). *J. Phys. Chem. C* **2013**, *117*, 9895–9902.
- (9) Greenwood, J.; Fruchtl, H. A.; Baddeley, C. J. Ordered growth of upright melamine species on Ni{111}: A study with scanning tunnelling microscopy and reflection absorption infrared spectroscopy. *J. Phys. Chem. C* **2012**, *116*, 6685–6690.
- (10) Ammon, C.; Bayer, A.; Held, G.; Richter, B.; Schmidt, T.; Steinrück, H. P. Dissociation and oxidation of methanol on Cu(110). *Surf. Sci.* **2002**, *507*, 845–850.
- (11) Pawlak, R.; Clair, S.; Oison, V.; Abel, M.; Ourdjini, O.; Zwaneveld, N. A. A.; Gignès, D.; Bertin, D.; Nony, L.; Porte, L. Robust supramolecular network on Ag(111): hydrogen-bond enhancement through partial alcohol dehydrogenation. *ChemPhysChem* **2009**, *10*, 1032.
- (12) Bebensee, F.; Svane, K.; Bombis, C.; Masini, F.; Klyatskaya, S.; Besenbacher, F.; Ruben, M.; Hammer, B.; Linderöth, T. Adsorption and dehydrogenation of tetrahydroxybenzene on Cu(111). *Chem. Commun.* **2013**, *49*, 9308–9310.
- (13) Simonsen, J. B. The interaction between hexahydroxytriphenylene and the rutile TiO₂(110)-(1 × 1) surface at UHV conditions. *Surf. Sci.* **2010**, *604*, 1300–1309.
- (14) Fischer, S.; Papageorgiou, A. C.; Lloyd, J. A.; Oh, S. C.; Diller, K.; Allegretti, F.; Klappenberger, F.; Seitsonen, A. P.; Reichert, J.; Barth, J. V. Self-assembly and chemical modifications of bisphenol A on Cu(111): interplay between ordering and thermally activated stepwise deprotonation. *ACS Nano* **2014**, *8*, 207–215.
- (15) Klappenberger, F. Two-dimensional functional molecular nanoarchitectures – Complementary investigations with scanning tunneling microscopy and X-ray spectroscopy. *Prog. Surf. Sci.* **2014**, *89*, 1–55.
- (16) Li, H.; Xu, B.; Evans, D.; Reutt-Robey, J. E. Isonicotinic acid molecular films on Ag(111): I. XPS and STM studies of orientational domains. *J. Phys. Chem. C* **2007**, *111*, 2102–2106.
- (17) Cossaro, A.; Puppin, M.; Cvetko, D.; Kladnik, G.; Verdini, A.; Coreno, M.; de Simone, M.; Floreano, L.; Morgante, A. Tailoring SAM-on-SAM formation. *J. Phys. Chem. Lett.* **2011**, *2*, 3124–3129.
- (18) Thebault, F.; Ohlström, L.; Haukka, M. 2,3,6,7,10,11-Hexahydroxytriphenylene tetrahydrate: a new form of an important starting material for supramolecular chemistry and covalent organic frameworks. *Acta Crystallogr., Sect. C: Cryst. Struct. Commun.* **2011**, *67*, o143–o145.
- (19) Andresen, T. L.; Krebs, F. C.; Thorup, N.; Bechgaard, K. Crystal structures of 2,3,6,7,10,11-oxytriphenylenes. Implications for columnar discotic mesophases. *Chem. Mater.* **2000**, *12*, 2428–2433.
- (20) Clair, S.; Abel, M.; Porte, L. Mesoscopic arrays from supramolecular self-assembly. *Angew. Chem., Int. Ed.* **2010**, *49*, 8237–8239.
- (21) Coratger, R.; Calmettes, B.; Abel, M.; Porte, L. STM observations of the first polymerization steps between hexahydroxytriphenylene and benzene-di-boronic acid molecules. *Surf. Sci.* **2011**, *605*, 831–837.
- (22) Marele, A. C.; Corral, I.; Sanz, P.; Mas-Balleste, R.; Zamora, F.; Yanez, M.; Gomez-Rodriguez, J. M. Some pictures of alcoholic dancing: from simple to complex hydrogen-bonded networks based on polyalcohols. *J. Phys. Chem. C* **2013**, *117*, 4680–4690.
- (23) Bocquet, F.; Nony, L.; Mannsfeld, S. C. B.; Oison, V.; Pawlak, R.; Porte, L.; Loppacher, C. Inhomogeneous relaxation of a molecular layer on an insulator due to compressive stress. *Phys. Rev. Lett.* **2012**, *108*, 206103.
- (24) Panaccione, G.; Vobornik, I.; Fujii, J.; Krizmancic, D.; Annese, E.; Giovanelli, L.; Maccherozzi, F.; Salvador, F.; De Luisa, A.; Benedetti, D.; et al. Advanced photoelectric effect experiment beamline at Elettra: A surface science laboratory coupled with Synchrotron Radiation. *Rev. Sci. Instrum.* **2009**, *80*, 043105.
- (25) Horcas, I.; Fernández, R.; Gómez-Rodríguez, J. M.; Colchero, J.; Gómez-Herrero, J.; Baro, A. M. A software for scanning probe microscopy and a tool for nanotechnology. *Rev. Sci. Instrum.* **2007**, *78*, 013705.
- (26) The origin of the small feature at lower BE can be assigned to first-layer molecules.
- (27) Its BE is sensibly lower than what is reported for a thick film of HHTP on TiO₂ (ref 13), probably because of a different energy level alignment at the interface in the two systems.
- (28) Phases P1 and P2 spectra were also measured by standard XPS (Mg K-α source, data not shown). The resulting A/B ratio was the same as that of higher resolution spectra.
- (29) Zhou, X.-L.; White, J. M.; Koel, B. E. Chemisorption of atomic hydrogen on clean and Cl-covered Ag(111). *Surf. Sci.* **1989**, *218*, 201.
- (30) Zhong, D. Y.; Franke, J. H.; Podiyanachari, S. K.; Blomker, T.; Zhang, H. M.; Kehr, G.; Erker, G.; Fuchs, H.; Chi, L. F. Linear Alkane polymerization on a gold surface. *Science* **2011**, *334*, 213–216.

(31) Aplincourt, P.; Bureau, C.; Anthoine, J. L.; Chong, D. P. Accurate density functional calculations of core electron binding energies on hydrogen-bonded systems. *J. Phys. Chem. A* **2001**, *105*, 7364–7370.

(32) Tu, G. D.; Tu, Y. Q.; Vahtras, O.; Agren, H. Core electron chemical shifts of hydrogen-bonded structures. *Chem. Phys. Lett.* **2009**, *468*, 294–298.

(33) Garcia-Gil, S.; Arnau, A.; Garcia-Lekue, A. Exploring large O 1s and N 1s core level shifts due to intermolecular hydrogen bond formation in organic molecules. *Surf. Sci.* **2013**, *613*, 102–107.

(34) O'Shea, J. N.; Schnadt, J.; Bruhwiler, P. A.; Hillesheimer, H.; Martensson, N.; Patthey, L.; Krempasky, J.; Wang, C. K.; Luo, Y.; Agren, H. Hydrogen-bond induced surface core-level shift in isonicotinic acid. *J. Phys. Chem. B* **2001**, *105*, 1917–1920.

(35) Schnadt, J.; Rauls, E.; Xu, W.; Vang, R. T.; Knudsen, J.; Laegsgaard, E.; Li, Z.; Hammer, B.; Besenbacher, F. Extended one-dimensional supramolecular assembly on a stepped surface. *Phys. Rev. Lett.* **2008**, *100*, 046103.

(36) Bisti, F.; Stroppa, A.; Perrozzi, F.; Donarelli, M.; Picozzi, S.; Coreno, M.; de Simone, M.; Prince, K. C.; Ottaviano, L. The electronic structure of gas phase croconic acid compared to the condensed phase: More insight into the hydrogen bond interaction. *J. Chem. Phys.* **2013**, *138*, 014308.

(37) Ref 33 showed that this effect is related to elongations and shortenings of C–O bond lengths in acceptors and donors, respectively.